



Supplementary Material for
**Spatiotemporal antagonism in mesenchymal-epithelial signaling in
sweat versus hair fate decision**

Catherine P. Lu, Lisa Polak, Brice E. Keyes, Elaine Fuchs*

*Corresponding author. Email: fuchs@rockefeller.edu

Published 23 December 2016, *Science* **354**, aah6102 (2016)
DOI: 10.1126/science.aah6102

This PDF file includes:

Figs. S1 to S8

Supplemental Figures

Fig. S1

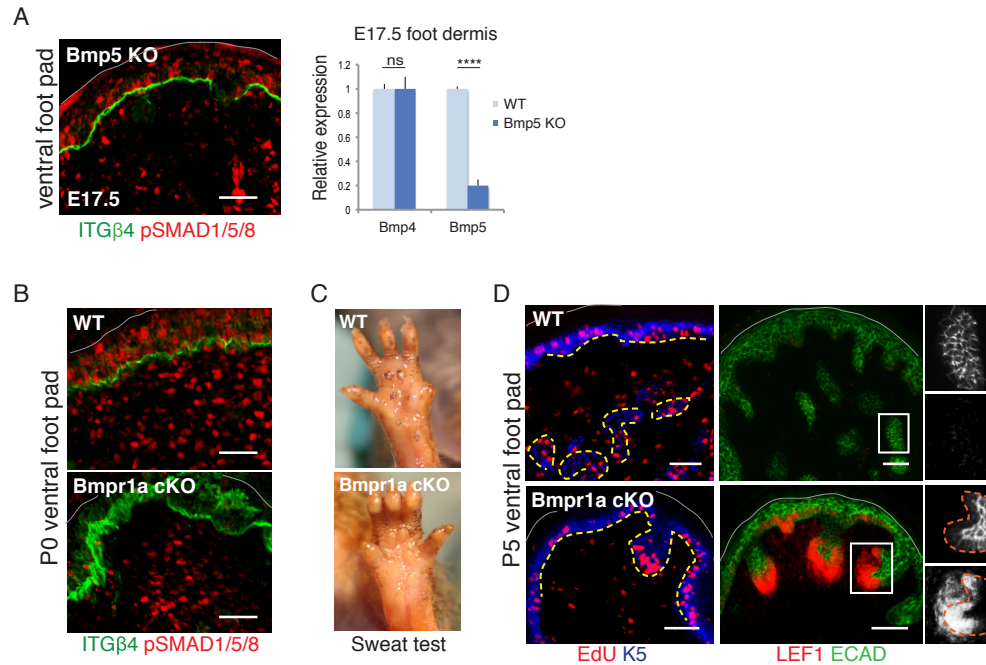


Fig. S1. Decreased mesenchymal BMP levels or the absence of epithelial BMP receptors impact fate determination of epidermal progenitors in ventral foot skin. **A**, Representative image of anti-phospho-Smad1/5/8 immunofluorescence on E17.5 foot skin lacking BMP5. When compared to WT (see Fig. 1D), BMP-signaling is significantly reduced. (Right) Quantitative PCR analyses showing decreased *Bmp5* expression in the *Bmp5*-null foot dermis, while *Bmp4* is still expressed at normal levels. N= 6-8 foot skin samples from 3-4 embryos. **B**, Immunofluorescence images showing complete loss of phospho-Smad1/5/8 signals in *K14-Cre; Bmpr1a* cKO foot epithelium, while still present in the dermis. **C**, Iodine-based sweat test showing loss of sweating function in *K14-Cre; Bmpr1a* cKO foot-skin. Fine black spots on foot pads indicate each actively sweating pore. **D**, Immunofluorescence images showing nucleotide analogue EdU (to mark proliferating cells) and nuclear LEF1 (to mark Wnt active cells) in the neonatal (P5) foot pads of WT and *K14-Cre; Bmpr1a* cKO mice. Split channels on the right highlight the absence of nuclear LEF1 in WT developing sweat glands, while nuclear LEF1 remains strong at the tip of growing HF's and adjacent DP. Together, these results are indicative of SwG to HF fate switching when competent epidermis is unable to respond to mesenchymal BMPs. Grey solid line marks the skin surface. Dashed lines, dermo-epidermal border. Boxed areas are shown in higher magnification at right. All scale bars, 50µm. Relevant to Fig. 1.

Fig. S2

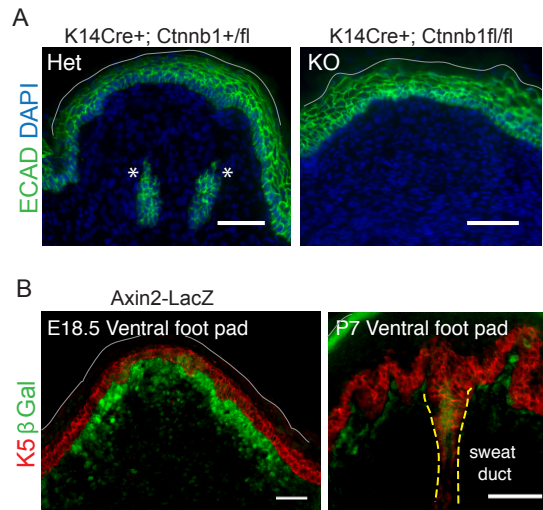


Fig. S2. In ventral foot pads, WNT/ β -catenin signaling is required for epidermal bud formation, but during the SwG-permissive phase, signaling is transiently elevated in mesenchyme and reduced in epithelium. **A**, Immunofluorescence images for *Krt14-Cre; Ctnnb1* Het (β -cat fl/+) and cKO (β -cat fl/fl) P0 mouse foot pads. Stars mark emerging sweat glands, absent when β -catenin is missing. Scale bars, 50 μ m. **B**, β -Galactosidase immunofluorescence images of E18.5 and P7 ventral foot pads of *Axin2-LacZ* WNT-reporter mice, showing strong WNT-responsive cells in the dermal region just beneath the epidermal-dermal border, characteristic of SwG-permissive skin (left). Also note that WNT-responsiveness is only transient within the sweat bud. It disappears as sweat buds invaginate and only reappears in the epidermis at later stages (P7) in the upper sweat duct (right). Grey solid lines mark the skin surface. Dashed lines, dermo-epidermal border. Scale bars, 50 μ m. Relevant to Fig. 4.

Fig. S3

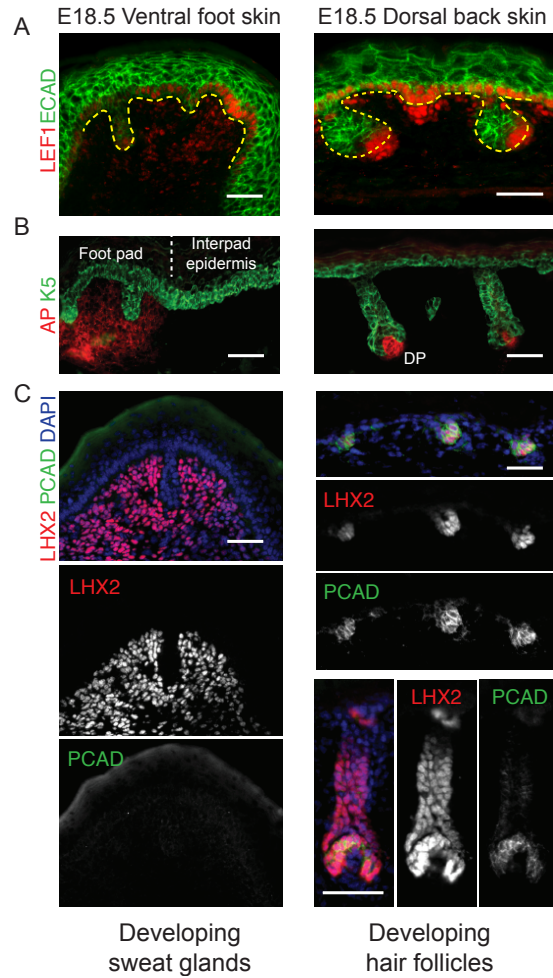


Fig. S3. Differences between ventral foot skin and dorsal back skin during fate permissive stages. Immunofluorescence images showing differential expression of WNT-effector DNA binding protein lymphoid enhancer factor 1 (LEF1), Alkaline phosphatase (AP), LHX2, and PCAD (DAPI in blue to mark chromatin). Note that **A**, Nuclear LEF1, a sign of active WNT-signaling, is present in epidermal buds of both foot skin (SwG) and back skin (HF), indicative of its importance in placode initiation. However, in sweat buds, nuclear LEF1 wanes during further invagination; while in hair buds, nuclear LEF1 is maintained at the down-growing tip. **B**, During the fate-permissive phase of foot skin, AP activity is transiently diffuse throughout the foot pad dermis (and not the inter-pad dermis); in back skin, AP is expressed in the dermal papillae (DP) of HFs. **C**, In foot skin, LHX2 expression is exclusively in the dermis, and PCAD is not upregulated in the sweat buds; in back skin, LHX2 and PCAD are both highly expressed in hair buds and pegs and is exclusive to the epithelium. Again, these differences were transient, waning after the fate-permissive phase. Scale bars, 50 μ m. Relevant to Fig. 4.

Fig. S4

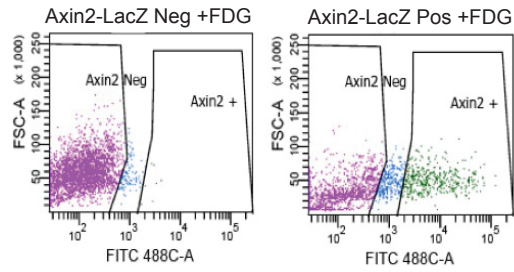


Fig. S4. FACS isolation of Axin2-LacZ-positive (β -galactosidase+) and Axin2-LacZ-negative dermal cells. *Axin2-LacZ*-negative embryonic dermal cells were used to establish the negative gate. FDG, fluorescein di-V-galactoside, was used to quantify intracellular β -galactosidase activity by flow cytometry. Relevant to Fig. 4.

Fig. S5

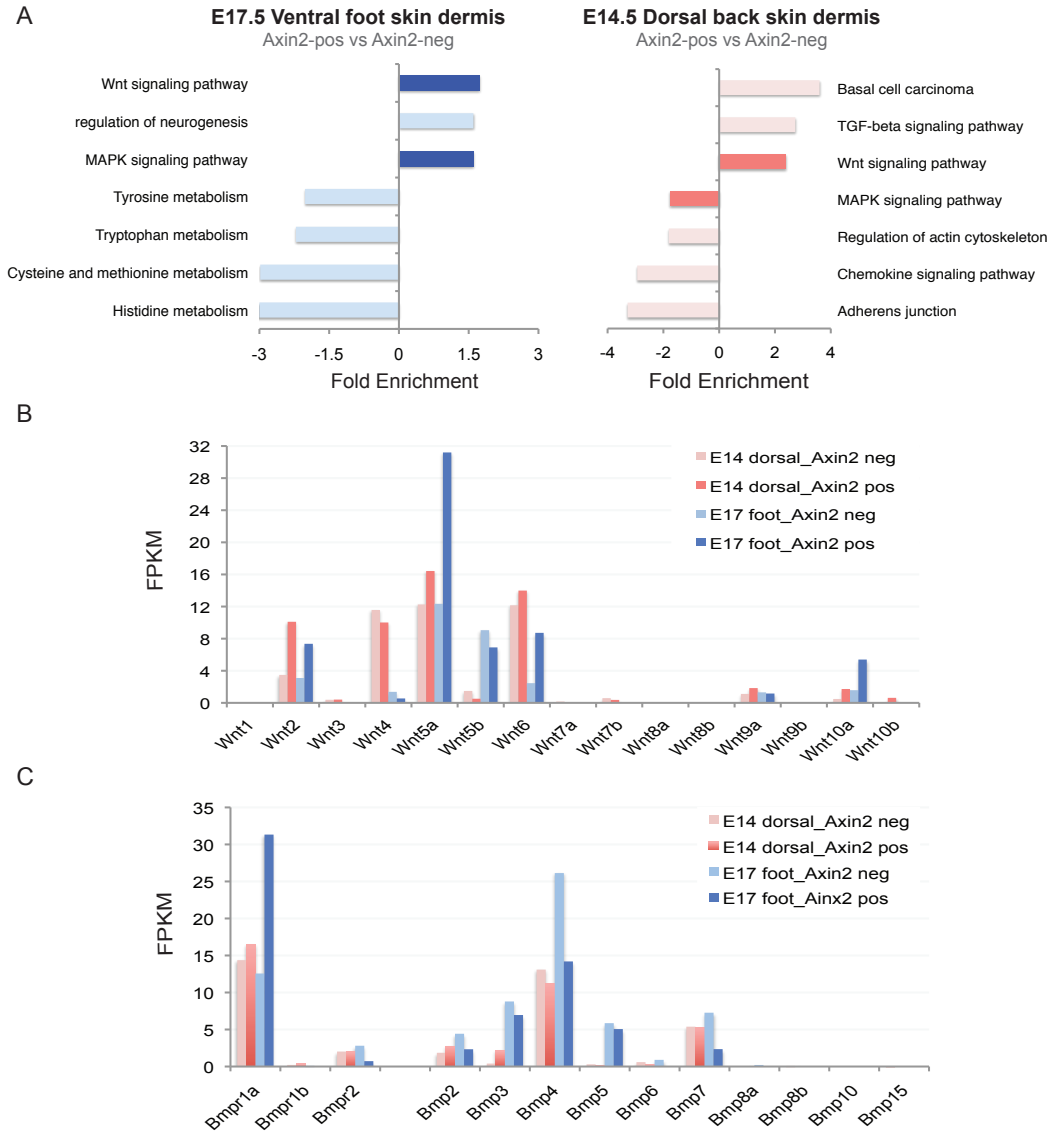


Fig. S5. Bioinformatic analysis of RNA-seq data. **A**, Gene Ontology (GO) term enrichment analysis from genes 2-fold different in ventral foot skin dermal AXIN2-positive versus AXIN2-negative cells (blue) and dorsal back skin dermal AXIN2-positive versus AXIN2-negative cells (pink). Note differences in WNT and MAPK signaling pathways between the two dermal populations. **B**, Expression of *Wnt* genes in cells as indicated from RNA-seq data. **C**, Expression of *Bmps* and *Bmp receptor* genes in cells as indicated from RNA-seq data. Relevant to Fig. 3.

Fig. S6

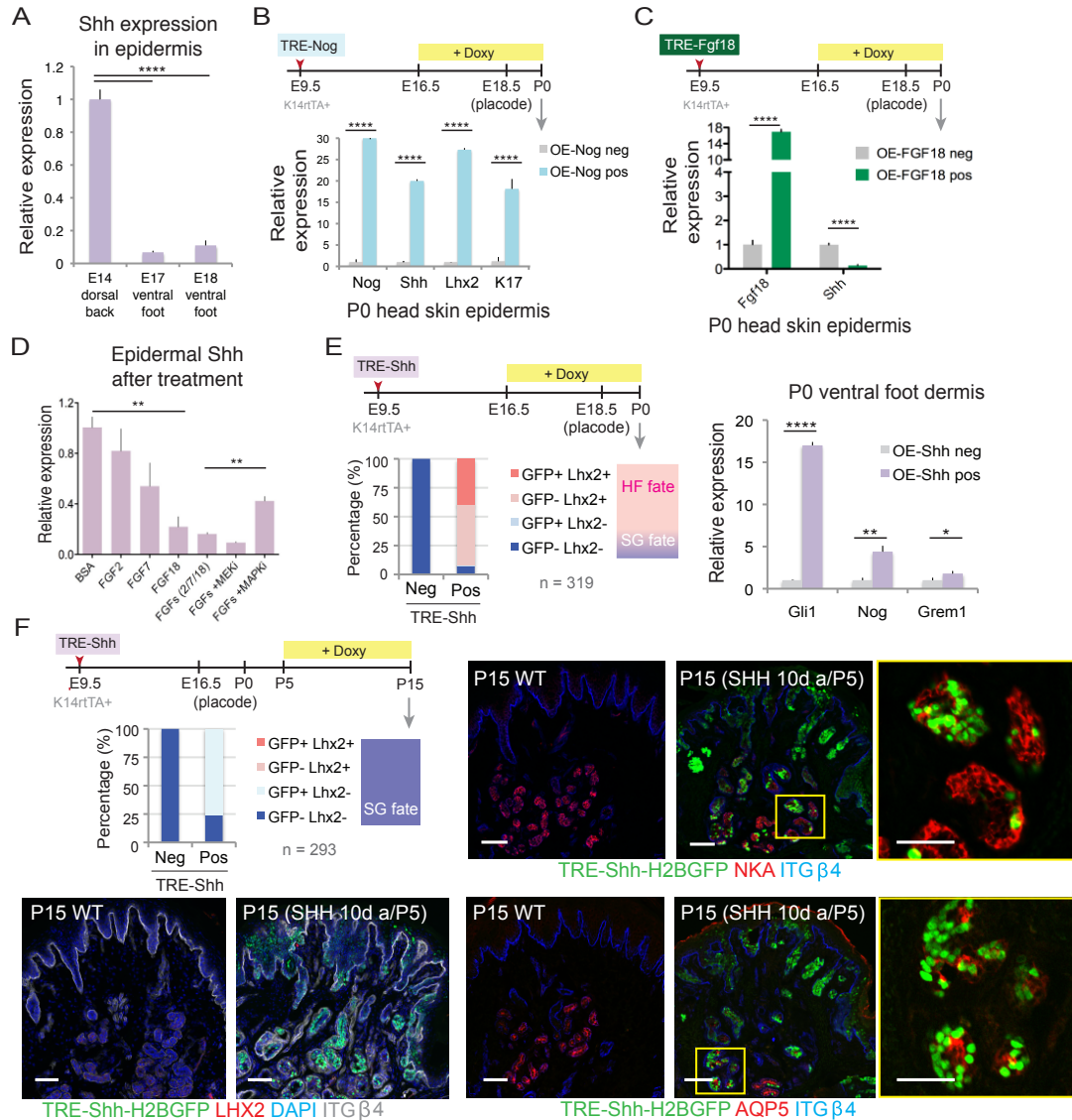


Fig. S6. SHH signaling is normally restricted to HF buds, but if administered during the critical window of fate-permissiveness, its activation in ventral foot skin, or repression in dorsal back skin, can elicit a switch in bud fates. **A**, Quantitative PCR for relative *Shh* expression in the epidermis of E14 dorsal back skin and E17 or E18 ventral foot skin, showing markedly low levels of *Shh* in the foot epidermis during sweat bud formation. **B**, Timeline of lentiviral injection, NOGGIN induction and analyses. Quantitative PCR showing upregulation of *Nog*, *Shh*, *Lhx2* and *Krt17* expression in LV-transduced back skin epidermis after doxy-induction of NOGGIN. **C**, Timeline of lentiviral injection, FGF18 induction and analyses. Quantitative PCR showing upregulation of *Fgf18* and suppression of *Shh* in LV-infected dorsal skin epidermis after doxy-induction of FGF18. **D**, *ex vivo* explant experiment with addition of FGFs and inhibitors (same experiment as shown in Fig. 6C). Quantitative PCR for *Shh* expression in foot skin epidermis after treatment. Note that FGF18 had the strongest effect in suppressing

Shh expression and the suppression could be partially rescued by MAPK inhibition. Experiments were performed twice, each with 6-8 pieces of E17.5 foot skin from 3 embryos. **E**, Timeline of lentiviral injection, SHH induction and analyses. Quantification of LHX2-positive and negative cells in the LV-transduced and non-transduced epidermis (cell number as indicated), showing that when SHH is elevated during early stages of epithelial bud formation, a switch from SwG to HF fate occurs as judged by HF epithelial marker LHX2 and as shown in the gradient color bar at right. Note that the SHH effect on fate change is more potent than NOGGIN (Fig. 3A). (Right) Quantitative PCR showing upregulation of *Gli1*, *Nog* and (modestly) *Grem1* in the dermis of the SHH-expressing foot skin. N=6-8 pieces of front foot skin from >3 embryos were collected for each experiment and analyzed. **F**, Timeline of lentiviral injection, SHH induction and analyses. Quantification of LHX2-positive and negative cells in the LV-transduced and non-transduced epidermis (cell number as indicated) and Immunofluorescence images, showing that when induction occurs after the epithelial bud stage, sweat gland fate is unaltered in the ventral foot skin. NKA and AQP5 are both markers of SwGs and remain expressed; LHX2, characteristic of HFs, was not induced. Boxed areas are shown in higher magnification at right. Scale bars, 50µm and 25 µm (far right). Relevant to Fig. 6.

Fig. S7

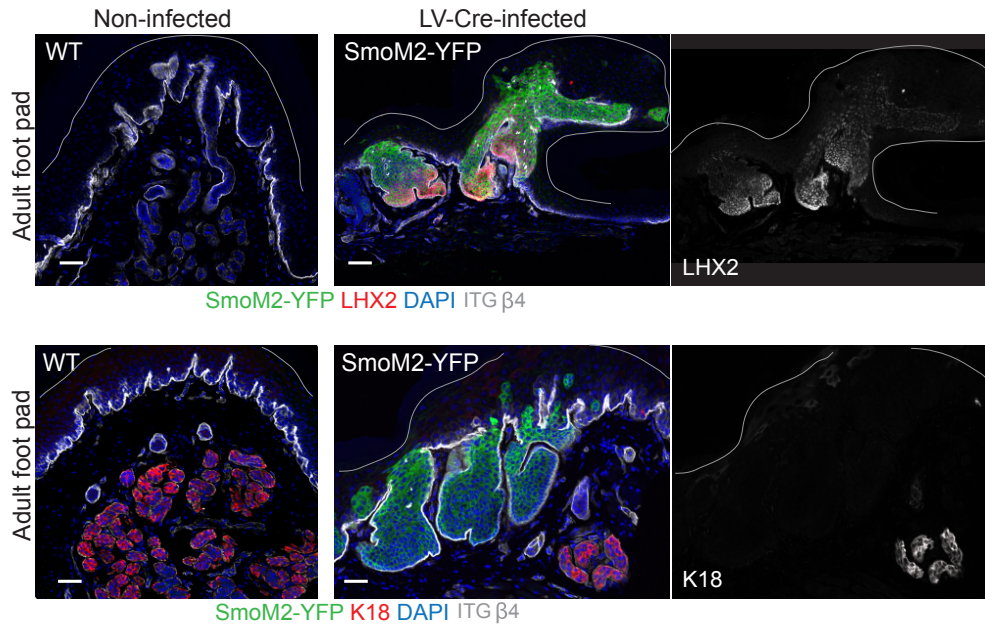


Fig. S7. SHH signaling within the foot skin epithelium is sufficient to alter fate during SwG development. Immunofluorescence images of LV-Cre transduced and non-transduced adult foot pad of *SmoM2-YFP*, a constitutive activator of SHH receptor signaling. Note that cells in YFP-positive patches express LHX2 and lack glandular morphology, while the remaining sweat glands (K18+) are YFP-negative. Grey solid lines denote skin surface. Scale bars, 50 μ m. Relevant to Fig. 6.

Fig. S8

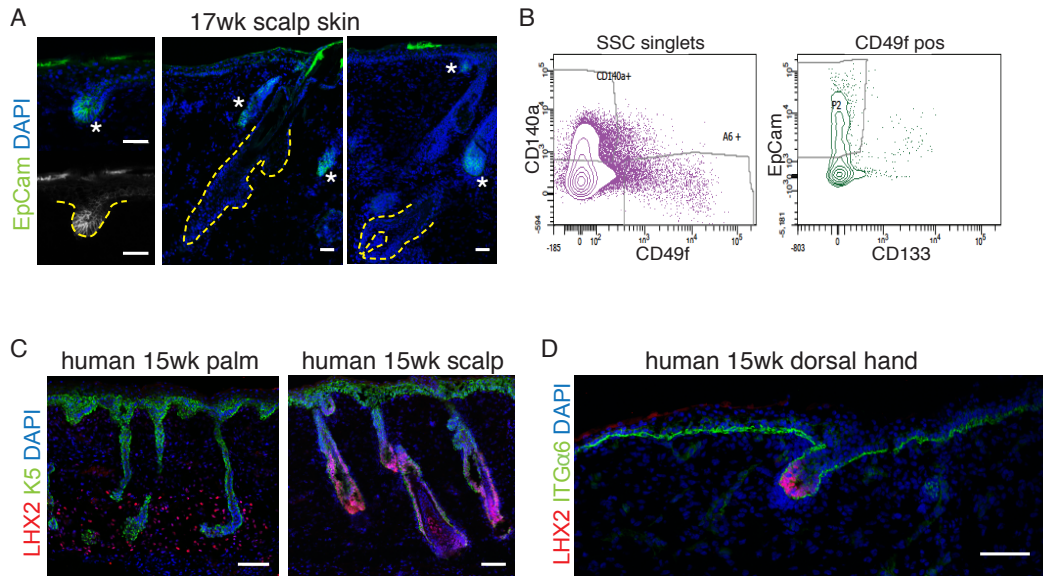


Fig. S8. FACS isolation of epidermal buds and dermal cells from human embryo scalp and palm skin. **A**, Immunofluorescence images for EpCam expression. Note that Epcam is only expressed at early epidermal buds (stars), not in mature HF. Dashed lines, dermo-epidermal border. Stars, EpCam-positive epidermal buds. Scale bars, 50 μ m. **B**, FACS sorting scheme. CD140a⁺ and CD49f⁺EpCam⁺ cells were collected for dermal and epidermal bud populations, respectively. **C-D**, Immunofluorescence images of LHX2 expression in human 15wk palm and scalp skin (**C**)(same image as in Fig. 7B), and 15wk dorsal side of hand (**D**). Note that similar to mouse, LHX2 expression is restricted to the HF's of dorsal skin, but to the dermis of ventral palm skin. Scale bars, 100 μ m. Relevant to Fig. 7.